Electrical and Optical Properties of Conducting Polymer with Quinoid Structure

Jpn. J. Appl. Phys. Vol. 36 (1997) pp. 3744–3749
Part 1, No. 6A, June 1997

Electrical and Optical Properties of Conducting Polymer with Quinoid Structure

Kazuhisa HOSODA, Kazuya TADA, Tsuyoshi KAWAI, Mitsuyoshi ONODA[1] and Katsumi YOSHINO

Department of Electronic Engineering, Osaka University, 2-1 Yamada-Oka, Suita, Osaka 565, Japan
[1]*Department of Electrical Engineering, Faculty of Engineering, Himeji Institute of Technology, 2167 Shosha, Himeji, Hyogo 671-22, Japan*

(Received November 21, 1996; accepted for publication April 1, 1997)

Poly[α-(bithiophene-5,5'-diyl)-(p-(heptyloxy)benzylidene)-co-(α-bithiophene quinodimethane-5,5'-diyl)] (PBTHBQ), which is obtained from precursor poly[α-(bithiophene-5,5'-diyl)-(p-(heptyloxy)benzylidene)] (PBTHB) by oxidative dehydrogenation with 2,3-dichloro-5,6-dicyano-p-benzoquinone and contains alternating aromatic and quinoid thiophene rings in its main chain, has an optical absorption edge at about 1.4 eV, while the band gap of PBTHBQ was evaluated to be about 2.6 eV from the short-circuited photocurrent spectrum. The electrochemical and optical properties of PBTHBQ and PBTHB have been investigated by cyclic voltammetry, *in situ* optical absorption spectroscopy, photoconduction spectra measurements and electron spin resonance measurements. From these experimental results, electronic energy states of PBTHBQ and PBTHB were estimated. PBTHBQ was also found to be made from PBTHB by an electrochemical cycle.

KEYWORDS: conducting polymer, electrochemical doping, aromatic structure, quinoid structure

1. Introduction

Conducting polymers with highly conjugated π-electron systems which can be doped chemically with strong electron acceptor or donor molecules, and demonstrate interesting physical phenomena such as an insulator-metal transition and electrochromism upon doping have attracted much interest from both fundamental and practical points of view. Various new concepts such as soliton, charged soliton, polaron and bipolaron have been introduced in order to explain the mechanism of these phenomena.[1–3] Proposals for various applications of conducting polymers also stimulated the synthesis of new types of conducting polymers.[4–7]

Among various conducting polymers, those composed of alternating aromatic and quinoid thiophene rings in their main chains are theoretically predicted to have small band gaps.[8] The conjugated polymers synthesized through the dehydrogenation process of precursor nonconjugated polymers are especially attractive as the functional polymers for application, since the precursor polymers are usually processable due to their solubility or fusibility. Several studies on soluble conjugated poly(heteroarylene methines) have been carried out.[9–12] However, the true electronic state of poly(heteroarylene methines) have never been clarified.

In this paper, we report the optical and electrochemical properties of poly[α-(bithiophene-5,5'-diyl)-(p-(heptyloxy)benzylidene)-co-(α-bithiophene quinodimethane-5,5'-diyl)] (PBTHBQ) synthesized through the dehydrogenation process of precursor nonconjugated polymer, poly[α-(bithiophene-5,5'-diyl)-(p-(heptyloxy)-benzylidene)] (PBTHB). Transformation of PBTHB to PBTHBQ by electrochemical doping is also demonstrated.

2. Experimental

PBTHBQ whose molecular structure is shown in Fig. 1 was synthesized by the oxidative dehydrogenation of PBTHB with 2,3-dichloro-5,6-dicyano-p-benzoquinone (DDQ), as reported by Chen *et al.*[12] Since the methine hydrogen resonance in the H-NMR spectra of PBTHBQ disappeared through the dehydrogenation process of precursor PBTHB, it is sure that conjugated polymer PBTHBQ was obtained. These polymers were dissolved in chloroform, and thin films were prepared by spin-coating the solution on the appropriate substrates. For electrical measurements, an indium-tin-oxide (ITO)-coated quartz plate was used as a substrate and an aluminum layer deposited by evaporation on the film was served as a second electrode.

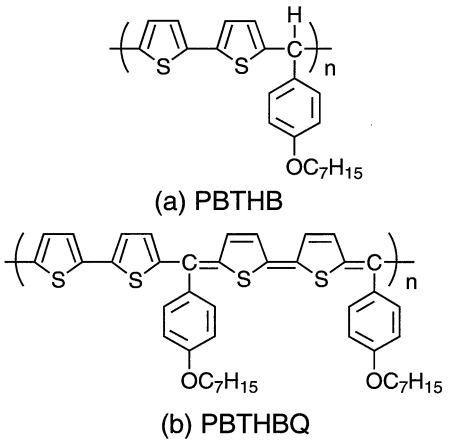

Fig. 1. Molecular structures of PBTHB and PBTHBQ.

A Fourier transform infrared spectrometer (Jasco FT/IR-300E) was used for absorption spectral measurements from 7000 to 650 cm^{-1} in wavenumber. A spectrophotometer (Hitachi 330) was used for *in situ* optical absorption spectral measurement during the electrochemical doping process with a potentiostat (Hokuto-Denko HA-501). Steady-state short circuit photocurrent in the spectral range from 800 to 300 nm was measured by irradiating the sample with a Xe arc lamp light passed through a monochromator. Cyclic voltammograms were obtained using a potentiostat (Hokuto-Denko HA-501) equipped with a programmable function generator (Hokuto-Denko HB-105) in an argon-filled dry box. A three-electrode cell with the polymer on an ITO-coated glass substrate as a working electrode, a silver

(Ag) wire as a reference electrode, a nickel (Ni) plate as a counter electrode and an acetonitrile (AN) solution containing tetrabutylammonium tetrafluoroborate ($TBABF_4$) as an electrolyte were used.

The optical absorption spectral changes during electrochemical doping were measured as follows. An electrochemical cell was constructed in the argon-filled dry box using a 1 cm pathlength quartz cuvette. The undoped polymer film on an ITO-coated quartz-glass substrate, a platinum wire counter and a silver wire reference electrodes were positioned inside the cuvette and used in a three-electrode cell system. The cell was filled with AN solution containing $TBABF_4$. The electrochemical potential of the polymer was determined relative to the Ag electrode.

The electron spin resonance (ESR) measurement was carried out as follows. A film of polymer of approximately 1 mg deposited on an ITO-coated glass substrate was doped in the same electrolyte and electrode construction as that used for the studies of cyclic voltammetry. In the dry box, the doped PBTHBQ film was washed rapidly with AN and placed in the ESR tube. The film in the ESR tube was dried in a vacuum. The ESR tube was placed in the resonance cavity of a spectrometer (Bruker ESP 300) and ESR was measured using the microwave power of 200 mW at X band at room temperature. The 1,1-diphenyl-2-picryl-hydrazyl (DPPH) served as a standard for the determination of absolute spin susceptibility (c), peak-to-peak linewidth (ΔHpp) and g value.

3. Results and Discussion

Figure 2 shows the FT-IR spectra of PBTHB and PBTHBQ film which was synthesized through the dehydrogenation process of PBTHB. PBTHBQ has a new absorption peak at around 1650 cm^{-1} which was not observed in the spectrum of PBTHB film. This is characteristic of the C=C ring stretching vibration in the quinoid bithiophene ring and the results are similar to those reported previously.[12] This indicates that PBTHB was certainly dehydrogenated to PBTHBQ.

Figure 3 shows the optical absorption (ultraviolet-visible-near-infrared) spectra of PBTHB film and chemically formed PBTHBQ film which was synthesized through the dehydrogenation process of PBTHB. The optical absorption spectrum of the precursor, PBTHB, only shows a single peak at around 3.8 eV. This peak is characteristic of the π–π^* absorption band of the aromatic bithiophene unit due to the HOMO-LUMO excitation. The absorption spectrum of PBTHBQ in the undoped state shows two major peaks. Because it is thought that the strong peak at about 3.8 eV may be the same as in the PBTHB absorption spectrum, the weak peak at about 2.1 eV should be attributed to the quinoid bithiophene units. There is also a novel shoulder at about 3.3 eV. Usually, band gap energy of the conducting polymer is evaluated roughly from the threshold wavelength of an absorption peak with lowest transition energy or exactly from the threshold energy of $(\alpha h\nu)^2$ vs $h\nu$ plot where α and $h\nu$ are the absorption coefficient and the photon energy, respectively.[13] The $(\alpha h\nu)^2$ vs $h\nu$ plot usually shows linear relationship at the threshold region and the intersection point of the regression line and the x-axis provides correct values of band gap energy. From the analysis of the threshold of the $(\alpha h\nu)^2$ vs $h\nu$ plot of the absorption peak at 2.1 eV, the band gap energy of PBTHBQ is estimated to be 1.4 eV, which is in agreement with previous papers.[9] However, in order to evaluate the band-gap energy, assignments of the absorption bands is necessary, since there could be not only the delocalized electronic band states but also some localized states. Origins of the optical transitions corresponding to the absorption peaks were investigated by two methods, measurements of short-circuit photocurrent of an ITO/PBTHBQ/Al and electrochemical absorptiometory.

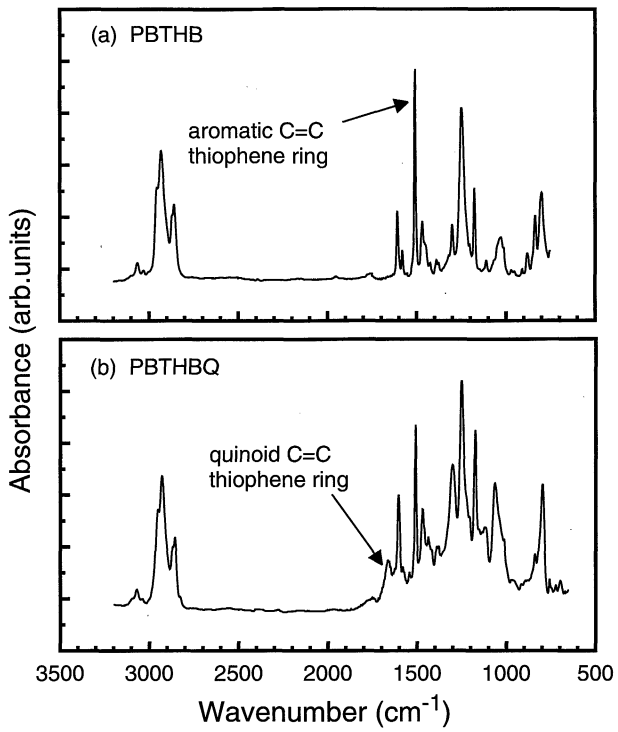

Fig. 2. FT/IR spectra of PBTHB and PBTHBQ films on NaCl plates at room temperature. (Wavenumber resolution = 2 cm^{-1})

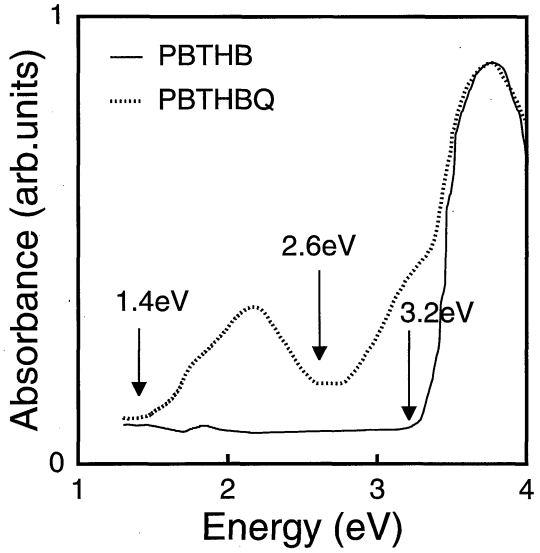

Fig. 3. Optical absorption spectra of PBTHB and PBTHBQ films on quartz plates at room temperature.

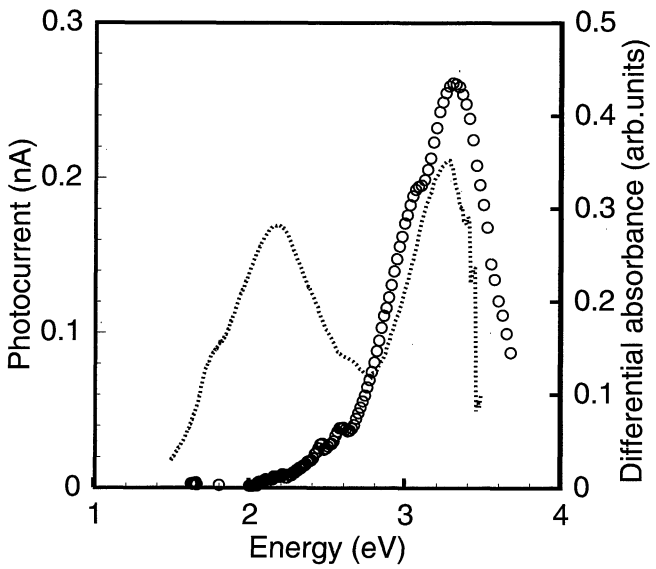

Fig. 4. Short-circuit photocurrent spectrum of ITO/PBTHBQ/Al cell at room temperature, where positive current corresponds to injections of electron from the polymer layer to the Al electrode and of hole from polymer layer to the ITO electrode. The gray line indicates the differential absorption spectrum of PBTHBQ film against PBTHB film.

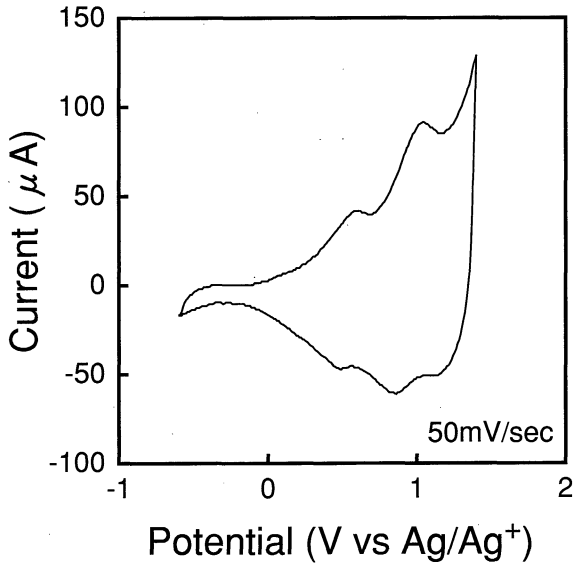

Fig. 5. Cyclic voltammogram of PBTHBQ film on an ITO substrate in $TBABF_4$/AN. (Scan rate = 50 mV/s)

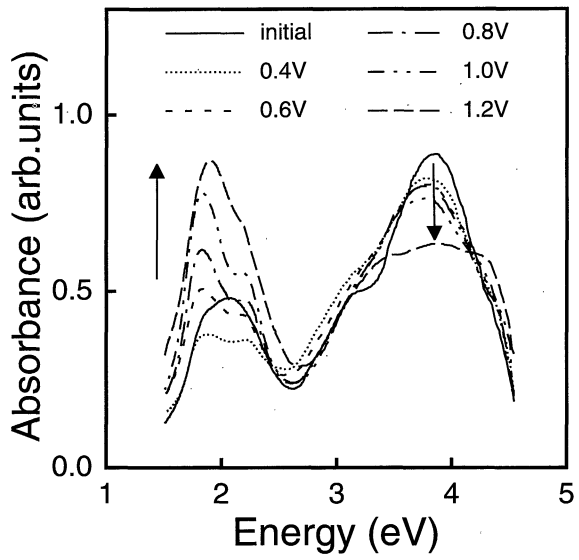

Fig. 6. Optical absorption spectral change of PBTHBQ film on an ITO substrate taken *in situ* during electrochemical BF_4^- doping as a function of the doping potential.

Figure 4 indicates the short-circuited photocurrent spectrum of an ITO/PBTHBQ/Al Schottky type cell, where only one peak was observed at around 3.3 eV. In this experiment, the current passing between ITO and Al electrodes was recorded upon monochromatic light irradiation. The photocurrent is explained to originate from the generation of mobile photocarriers on the polymer main chain and injections of positive and negative charge carriers from the polymer layer to the Al and the ITO electrodes, respectively. Since the polymer layer in this cell was approximately 0.2 μm in thickness, the light irradiated to the transparent ITO electrode seems to penetrate through the whole polymer layer to the Al electrode interface. In such a case, the photocurrent spectrum is expected to show a maximum at the peak energy of absorption band of the band gap excitation. The peak energy of the photocurrent spectrum coincided with that of one of peaks in differential absorption spectrum of PBTHBQ and PBTHB, which is also shown in Fig. 4. In this differential absorption spectrum, there are two peaks at 2.1 eV and at 3.3 eV and the former peak seems to give no marked photocurrent signal.

Figure 5 shows a typical cyclic voltammogram of a thin film of PBTHBQ in the potential range of -0.6 to $+1.4$ V vs Ag/Ag^+ at the sweep rate of 50 mV/s. The doping threshold potential is approximately 0.3 V vs the Ag/Ag^+. The Coulombic efficiency was almost 90%, which indicates a high degree of electrochemical reversibility of PBTHBQ. The redox reaction was accompanied by a reversible color change. Figure 6 shows the evolution of the optical absorption spectrum of PBTHBQ taken *in situ* during electrochemical BF_4^- doping as a function of the doping potential. The optical absorption spectrum of PBTHBQ in the undoped state showed two major peaks at about 3.8 eV and 2.1 eV. As the doping proceeded, the absorption peak at 3.8 eV was suppressed, while the absorption peak at 2.1 eV exhibited much different behavior. This peak was also slightly suppressed at first until the applied potential reached about 0.4 V (vs Ag/Ag^+), then increased with two new absorption peaks at 2.2 eV and 1.8 eV, and these peaks increased as the doping proceeded. Although the origin of this suppression of the absorption peak below 0.4 V vs Ag/Ag^+ electrode is not clear at this stage, it may correspond to the small side peak at about 0.5 V vs Ag/Ag^+ in the cyclic voltammogram shown in Fig. 5.

On the basis of these results, we evaluate the origins of the absorption bands. Usually, the band gap transition generates positive and negative charge carriers which contribute to the photoconduction and also to the photovoltaic effect at the Schottky junction. That is, upon photoexcitation of band gap transition, the negative and positive charge carriers generated in the conducting poly-

mers are expected to migrate through the conducting polymer layer to the polymer-electrode interfacial regions and/or to be injected into the ITO and Al electrodes, respectively, resulting in short-circuit photocurrent. On the other hand, the absorption band corresponding to the band gap transition should be suppressed upon electrochemical doping, since it should decrease the number of electron in the valence band and also the transition probability. These typical natures of band gap transition can not be seen in the absorption peak at 2.1 eV. That is, there is no clear photocurrent peak corresponding to the optical absorption peak at around 2.1 eV. There is a possibility that the photocurrent signal corresponding to the absorption peak at 2.1 eV is too weak to detect, even if this absorption peak would correspond to the band gap transition. However, upon the electrochemical p-type doping, the absorbance at about 2 eV did not decrease but increased as shown in Fig. 6, while that at about 3.8 eV was suppressed markedly. These electrochemical observations clearly indicated that the absorption peak at 2.1 eV does not correspond to the band gap transition while that at 3.8 eV and/or the absorption shoulder at 3.3 eV behave as the band gap transition. Since the peak energy of the photocurrent signal coincides with one of the peaks of the differential absorption spectrum shown in Fig. 4, the absorption band at about 3.3 eV is thought to be the band gap transition. That is, chemical dehydrogenation of PBTHB to PBTHBQ forms an extensively conjugated π-electron system and a delocalized electronic band structure, which shows a novel band gap absorption band at about 3.3 eV as a side band of the absorption peak at 3.8 eV of the aromatic bithiophene unit. Though the origin of the absorption peak at 2.1 eV is not clear at this moment, the excited state generated by this transition seems to be localized at the excitation region, since it does not contribute to the photocurrent. Accordingly, it is considered that the band gap of PBTHBQ is not 1.4 eV which was the value obtained from evaluation of the tail of the absorption peak of 2.1 eV.

To obtain the correct value of the band gap energy, we need to evaluate the threshold energy of the absorption peak at 3.8 eV or the shoulder at 3.3 eV. About 2.6 eV was obtained as the threshold energy of the $(\alpha h\nu)^2$ vs $h\nu$ plot of the absorption peak at 3.8 eV, although this value contains considerable amount of probably error since the overlapping peak at 2.1 eV hides the true threshold energy of the $(\alpha h\nu)^2$ vs $h\nu$ plot. However, the $(ih\nu)^2$ vs $h\nu$ plot, where i is the photocurrent signal, showed a clear linear region at about 2.8eV and the regression line intersects with the $(ih\nu)^2 = 0$ line at 2.6 eV. The remarkable tail of the photocurrent spectrum at about 2.2 eV may be attributed to the tail of the absorption band at 3.8 eV or the shoulder at 3.3 eV which seems to be hidden by the strong absorption band at 2.1 eV. Therefore, the correct value for the band gap energy of PBTHBQ is estimated to be about 2.6 eV.

As described above, PBTHBQ has interesting and complex characteristics. The electrochemical and optical properties of precursor PBTHB have also been investigated. Figure 7 shows the cyclic voltammogram of PBTHB film doped at various doping potential range.

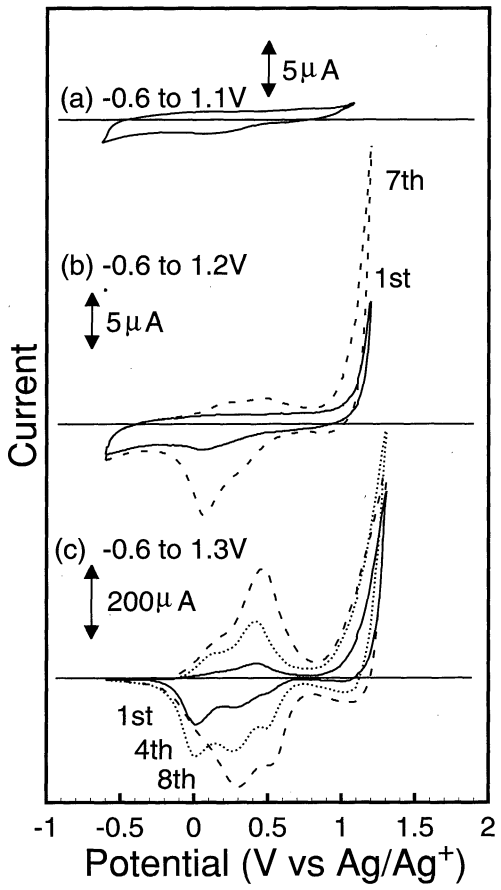

Fig. 7. Cyclic voltammogram of PBTHB film on an ITO substrate in $TBABF_4$/AN at various doping potential range with the scan rate of 50 mV/s.

Data were taken for several cycles at the sweep rate of 50 mV/s. Initially, the scan range was set from −0.6 to 1.1 V (Fig. 7(a)), then the higher potential was applied up to 1.2 V (Fig. 7(b)) and 1.3 V (Fig. 7(c)). In the scan range from −0.6 to 1.1 V, no current was observed and the film of PBTHB remained almost transparent. By the scanning in the range from −0.6 to 1.2 V current waves were found to increase from the doping potential of about 0.9 V (vs Ag/Ag^+) and with the repetition of cycles, the doping and undoping current of PBTHB film increased gradually. Moreover, when the highest potential was increased to 1.3 V, the color of PBTHB film also began to change while the current waves increased gradually with the repetition of cycles as shown in Fig. 7. That is, the film was speckled in blue, and many branches extended from the speckles with repeated doping and undoping. Finally, the film became dark blue. This color change was observed especially at the higher potential of more than about 1.0 V (vs Ag/Ag^+). After the entire PBTHB film was colored, its color changed to green in the undoped state at −0.6 V, and returned to dark blue in the doped state at 1.3 V. This color change is just same as that of PBTHBQ film.

A constant potential between 0.8 V and 1.3 V (vs Ag/Ag^+) was applied to the PBTHB film for about 15 min in the solvent of a AN containing $TBABF_4$. For voltage lower than 0.9 V, no changes were observed, but the film changed to blue in color at the constant po-

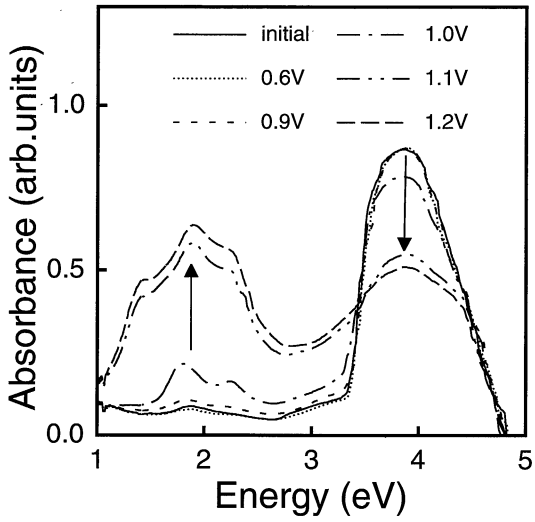

Fig. 8. *In situ* optical absorption spectra of PBTHB as a function of the doping potential against the Ag reference electrode measured in $TBABF_4$/AN solution.

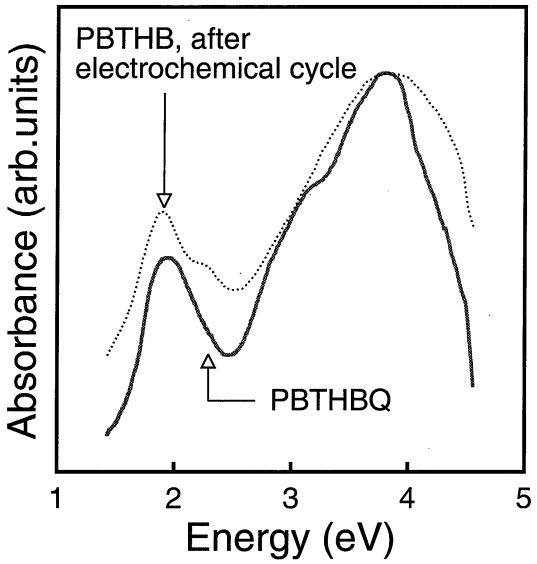

Fig. 9. Optical absorption spectra of PBTHB (dedoped state after an electrochemical doping cycle) and pristine PBTHBQ.

tential of 1.0 V, and gradually darkened with increase of the applied potential. The color of PBTHB film after electrochemical doping did not return to that of the initial state, even exposure to ammonia vapor. That is, the color change of the film from transparent (initial PBTHB) to dark blue is not a reversible phenomenon. The dark blue color might be interpreted to be that of doped PBTHBQ.

The evolution of the absorption spectra of PBTHB during electrochemical doping with about 1.0 V (vs Ag/Ag^+) has also been studied *in situ*. Figure 8 shows the optical absorption spectral change of BF_4^- doped PBTHB at various doping potentials in $TBABF_4$/AN. The absorption spectrum of PBTHB in the undoped state showed single peak at 3.8 eV due to HOMO-LUMO excitation at the aromatic bithiophene units. As the doping proceeds, the interband absorption peak is suppressed, whereas two new absorption peaks appear simultaneously at about 2.2 eV and 1.8 eV where characteristic peaks were observed in the PBTHBQ film at high doping potential as shown in Fig. 6. These peaks become larger with increased applied potential. The color of the PBTHB film also changed from transparent (in the undoped state) to dark blue (in the doped state).

When the PBTHB was dedoped, the peaks at around 2 eV did not disappear completely. That is, the electrochemical doping effect of PBTHB was irreversible. As shown in Fig. 9, the optical absorption spectrum of PBTHB dedoped at 0 V (vs Ag/Ag^+) for a long period was similar to that of undoped (neutral) PBTHBQ in $TBABF_4$/AN obtained by the chemical dehydrogenation method.

The absorption spectrum of this electrochemically treated PBTHB exhibited similar characteristics to those of PBTHBQ when it was doped again. This indicates that some bithiophene was transformed from the aromatic structure to the quinoid structure by the electrochemical hydrogenation. Since the electrolyte solution was dried carefully before use, there was almost no water and the protons which were eliminated from the PBTHB upon the electrochemical reaction diffused within the electrolyte solution and were hard to react with the polymer upon the reverse scan, forming the quinoid forms.

The magnetic properties of electrochemically treated PBTHB also exhibited characteristics similar to those of PBTHBQ. In the undoped PBTHBQ, spin susceptibility (χ) and linewidth (ΔHpp) are about 6.2×10^{18} spins/g and about 6.3 G, respectively. Assuming a Curie spin contribution, χ evaluated in the undoped PBTHBQ corresponds to approximately one unpaired spin per about 250 units. PBTHBQ has a relatively higher spin density in comparison with the undoped polythiophene whose χ is about 1×10^{18} spins/g.[4] This result indicates that the formation of the structural defects in the chemical dehydrogenation of PBTHB to produce PBTHBQ.

Figure 10 shows ESR signals of pristine PBTHB and PBTHB which is in a dedoped state after electrochemical doping. The relative intensity of the ESR signals changed remarkably after electrochemical doping. The ESR spin density of the pristine PBTHB was about 1.0×10^{17} spins/g and that of dedoped PBTHB was 1.0×10^{18} spins/g, which is similar to that of chemically dehydrogenated PBTHBQ in the undoped state. From this measurement, the formation of the structural defects was confirmed to some degree, though the PBTHB film was dedoped. This change of the intensity of the ESR signals might be explained as the removal of methine protons of PBTHB upon the electrochemical cycle and PBTHB changed structurally to the conducting polymer PBTHBQ, and coincides with the result shown in Fig. 7. Since the relative intensity of the absorption peak at about 2 eV against the absorption peak at 3.8 eV coincided roughly with that of PBTHBQ as shown in Fig. 9, the number of quinoid form generated by the electrochemical cycle seems to correspond to the number of the aromatic formafter the electrochemical cycle and the structure of PBTHB after the electrochemical cycle should be similar to that of PBTHBQ as shown in Fig. 1. Comparison between electricity upon the electrochemical conversion process with the progress of the

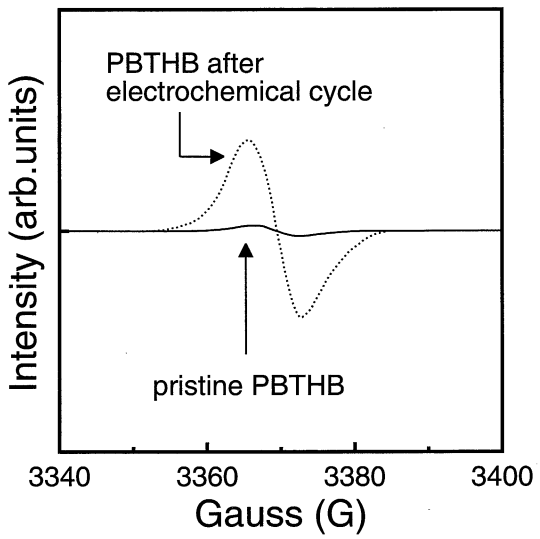

Fig. 10. ESR signals of PBTHB before anf after the electrochemical cycle.

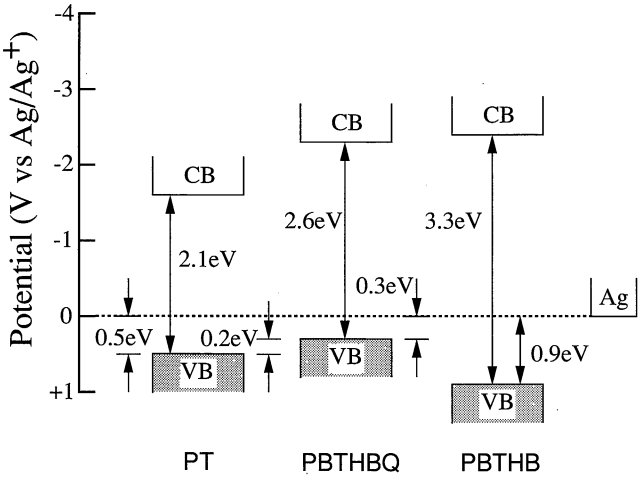

Fig. 11. Electronic energy level diagrams of PBTHB and PBTHBQ.

formation of quinoid structure was unsuccessful which indicated that some electrochemical side reaction may exist.

The electronic energy structures of PBTHB and PBTHBQ were evaluated as illustrated in Fig. 11. In the undoped state, the band gaps of PBTHB and PBTHBQ are 3.3 eV and 2.6 eV respectively. The top of the valence band of PBTHB and PBTHBQ estimated from the doping threshold potential is almost 0.9 V (vs Ag/Ag^+), and 0.3 V (vs Ag/Ag^+) respectively. It should be noted that the top of the valence band of PBTHBQ is located at higher energy than that of PT by 0.2 eV.[14] The result suggests that the dopant in PBTHBQ is relatively stable compared with that in PT.

4. Summary

The present experimental results concerning PBTHB and PBTHBQ which has been reported as a narrow band gap conducting polymer can be summarized as follows.

(1) The optical absorption spectrum of the undoped PBTHBQ showed two major absorption peaks at about 3.8 eV and 2.1 eV. while the short circuit photocurrent spectrum showed a clear peak at 3.3 eV. These results indicated that the absorption peak at about 2.1 eV corresponds not to the band gap excitation but to a localized excitation.

(2) In a cyclic voltammogram of PBTHBQ, the redox reaction accompanies a reversible color change. The Coulombic efficiency of PBTHBQ was higher than 90%, which is indicative of a high degree of electrochemical reversibility. The doping threshold potential of PBTHBQ was located at about 0.3 V (vs Ag/Ag^+), which is higher than that of PT by about 0.2 eV.

(3) *In-situ* optical absorption measurements of PBTHBQ during electrochemical doping showed that the peak at about 3.8 eV was suppressed and the peak at around 2 eV increased simultaneously, suggesting that the peak at about 3.8 eV corresponded to the band gap excitation. From the threshold energy of the $(\alpha h\nu)^2$ vs $h\nu$ plot, the band gap energy was evaluated to be about 2.6 eV, which indicates that the PBTHBQ is not a small band gap conducting polymer.

(4) By electrochemical treatment of PBTHB with potential higher than 1.0 V (vs Ag/Ag^+), PBTHB showed similar voltammetric and electrochromic properties as PBTHBQ.

(5) In the magnetic properties, dedoped PBTHB after electrochemical doping and dehydrogenated PBTHB showed a spin density of the same order ($\times 10^{18}$ spins/g), which had many structural defects.

(6) From the results of (4) and (5), it was assumed that PBTHBQ could be synthesized by electrochemical dehydrogenation of PBTHB.

Acknowledgements

This work was partly supported by the Research for the Future Program of the Japan Society for the Promotion of Science (Project No. JSPS-RFTF96P00206) and by a Grant-in-Aid for Scientific Research (A) from the Ministry of Education, Science, Sports and Culture.

1) W. P. Su, J. R. Schrieffer and A. J. Heeger: Phys. Rev. Lett. **42** (1979) 1698.
2) S. N. Chen, A. J. Heeger, Z. Kiss, A. G. MacDiarmid, S. C. Gau and D. L. Peebles: Appl. Phys. Lett. **36** (1980) 96.
3) J. L. Bredas, B. Themans and J. M. Ande: Phys. Rev. B **27** (1983) 7827.
4) K. Yoshino, K. Kaneto and Y. Inuishi: Jpn. J. Appl. Phys. **22** (1983) L157.
5) K. Yoshino, M. Tabata, K. Kaneto and T. Ohsawa: Jpn. J. Appl. Phys. **24** (1985) 9.
6) K. Yoshino, R. Sugimoto, J. G. Rabe and W. F. Schmidt: Jpn. J. Appl. Phys. **24** (1985) L33.
7) M. Onoda, S. Morita, H. Nakayama and K. Yoshino: Jpn. J. App. Phys. **32** (1993) 3534.
8) J. M. Toussaint and J. L. Bredas: Macromolecules **26** (1993) 5240.
9) S. A. Jenekhe: Macromolecules **19** (1986) 2663.
10) H. Braunling, R. Becker and G. Blochl: Synth. Met. **41** (1991) 1539.
11) W. C. Chen and S. A. Jenekhe: Macromolecules **28** (1995) 454.
12) W. C. Chen and S. A. Jenekhe: Macromolecules **28** (1995) 465.
13) M. Onoda, Y. Manda, T. Iwasa, H. Nakayama, K. Amakawa and K. Yoshino: Phys. Rev. B **42** (1990) 11826.
14) K. Kaneto, S. Takeda and K. Yoshino: Jpn. J. Appl. Phys. **24** (1985) L553.